Proc. of SPIE Vol. 3132, Optomechanical Design and Precision Instruments, ed. A E Hatheway (Oct 1997) Copyright SPIE

Detector mount system for thermal isolation

Mark T. Sullivan[a], Matthew R. Bye[a], Paul D. Ehrensberger, Jr[a], Enrique Romero[a], Howard P. Demroff[b], Scott C. Fletcher[b], Daniel B. DeBra[c], John H. Goebel[d], Paul K. Limtiaco[a], Donald E. Davidson[e], Lynn W. Huff[b], Ada M. Jefferson[b], Ali Kashani[f], Dale K. Gill[a], Kenneth J. Triebes[b], Jeffrey A. Grant[a]

[a]W. W. Hansen Experimental Physics Laboratory, Stanford University, Stanford, CA 94305
[b]Advanced Technology Center, Lockheed Martin Missiles and Space, 3251 Hanover Street, Palo Alto, CA 94304
[c]Aeronautics and Astronautics Department, Stanford University, Stanford, CA 94305
[d]Sensors and Instrumentation Branch, NASA Ames Research Center, Moffett Field, CA 94035
[e]Optical Instrument Design, 7371 Hyssop Drive, Etiwanda, CA 91739
[f]Atlas Scientific, 713 San Conrado Terrace, Sunnyvale, CA 94086

ABSTRACT

This paper describes the design, fabrication, and testing of a low-temperature detector mount system which provides thermal isolation between detector electronics, operating at 80 kelvins, and a quartz telescope at 2.5 kelvins. The detector will be used to acquire and track the guide star for the Gravity Probe B Relativity Mission. The detector mount makes use of flex circuit technology for the critical thermal isolator. The detector mounts are configured in a redundant manner through the use of a beamsplitting optic. The entire package mounts to a quartz post through a semi-kinematic mount. Design consideration is given to electromagnetic interference and low-remanent magnetic moment. The detector mounts use a flex cable for electrical connections, as well as thermal grounding. The principal benefit of this design is the ability to operate relatively warm pre-amplifier electronics in a low-temperature environment with minimal disruption to a cryogenic system. Test results have shown this detector mount capable of dissipating less than 2 milliwatts with an 80 K temperature differential.

Keywords: low-temperature, detector, thermal conductivity, polyimide, flex circuit, kinematic, telescope, Gravity Probe B

1. INTRODUCTION

Gravity Probe B (GP-B) is a relativity experiment to measure the geodetic and frame-dragging precessions of a gyroscope placed in a 650 km altitude polar orbit about the Earth. The measurements are to be made relative to an inertial reference frame provided by the fixed stars. For Einstein's general relativity, the precessions are calculated to be 6.6 arc seconds/year for the geodetic precession and 0.042 arc seconds/year for the frame-dragging precession. The goal of the GP-B experiment is to measure these precessions to better than 0.01% and 1%, respectively[1].

To perform these measurements, the GP-B Science Instrument (Figure 1) consists of four quartz gyroscopes aligned in a fused quartz block. A fused quartz, star-tracking telescope is attached to the block and orients the Instrument by tracking a guide star. A sensitive, superconducting sensor is used to accurately measure the axis of rotation of each gyroscope with respect to the quartz block[2]. This information is compared with the absolute angle reference provided by the telescope and its read-out electronics. The Science Instrument is operated in a cryogenic, low-noise environment provided by a low vacuum ($<10^{-13}$ torr), a superfluid, liquid helium (LHe) dewar operating at 2.5 K, superconducting shielding, and a drag-free satellite. A pure gravitational orbit for the satellite is determined by using displacement signals derived from the gyroscope suspension system. This gyroscope acts as a drag-free proof mass.

The star-tracking telescope is a modified-Cassegrain design with a 144 mm aperture, an overall length of 505 mm, and a focal length of 3810 mm (f/27). The telescope has an ellipsoidal primary mirror, a spherical secondary mirror, and a spherical tertiary mirror. Starlight enters the telescope through a forward plate, proceeds through the imaging optics, then is

Further information –
M.T.S. (correspondence): Email: marks@blueshift.stanford.edu; Telephone: (650)723-3367

sent to an Image Divider. A beamsplitter splits the photon beam. These two beams fall onto two, sharp, roof-edge prisms which split each beam again. The two sets of divided light, now four separate beams, proceed to two, dual photodiode detectors. By measuring the relative intensities of each of the two beam pairs, the telescope read-out electronics tell the spacecraft attitude control system how much to adjust the spacecraft orientation. One detector set senses light intensity for pitch position. The other set senses light intensity providing yaw position. The GP-B star-tracking telescope will provide an inertial reference for the Science Instrument with accuracy approaching 100 micro-arc seconds/year[3].

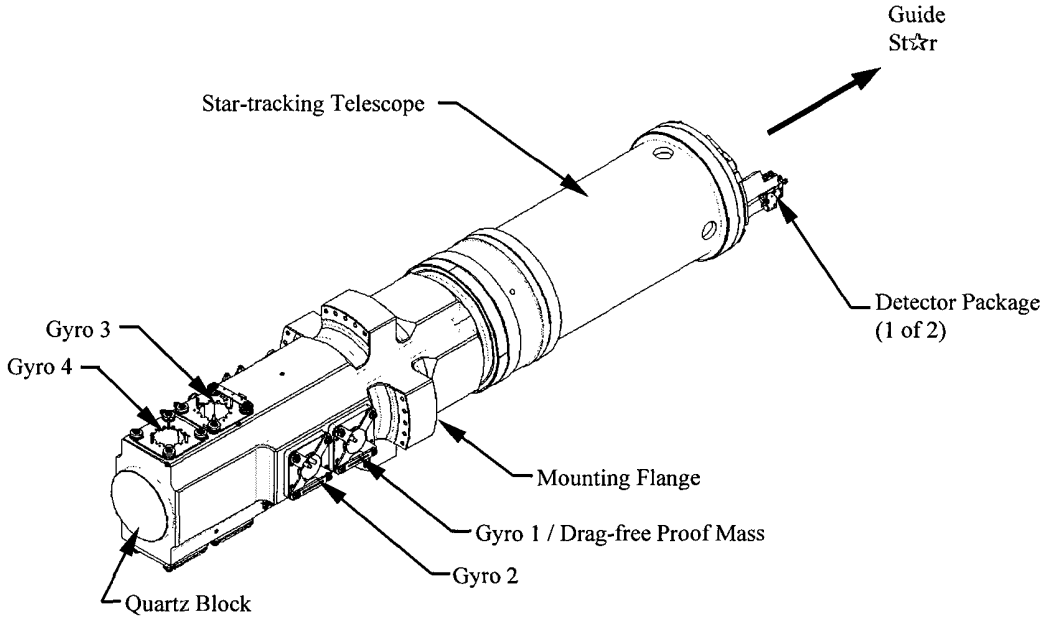

Figure 1. The Gravity Probe B Science Instrument Four gyroscopes are positioned along an axis in a fused quartz block The fused quartz telescope orients the GP-B spacecraft by tracking a guide star

As shown in Figure 2, GP-B Detector Packages are 90 degrees apart to receive light from the Image Divider. The Detector Packages must be compatible with the all-quartz, cryogenic telescope and not obscure the clear aperture. Detector electrical signals flow through cables and connectors to the dewar probe (not shown).

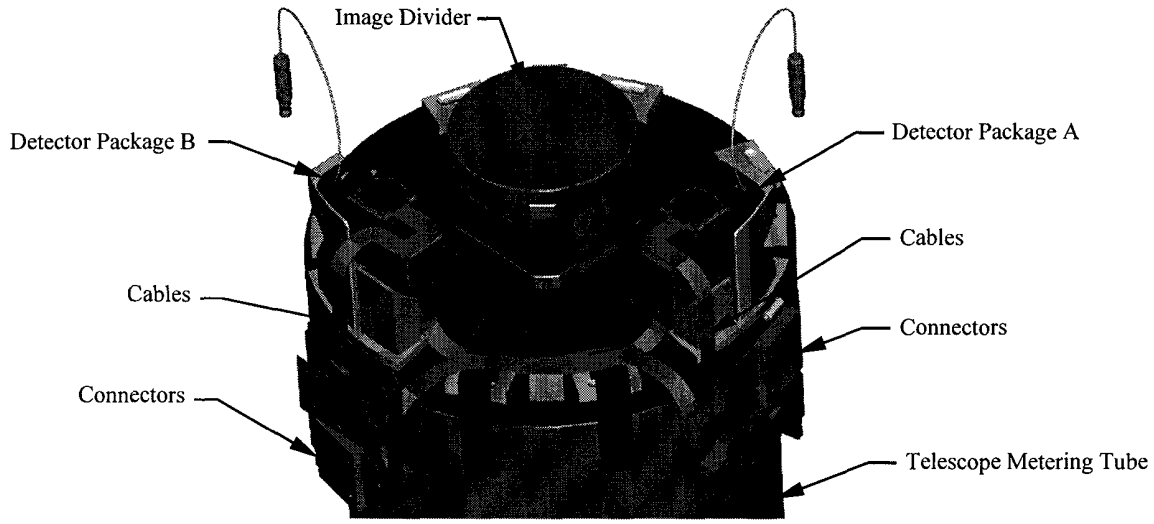

Figure 2. Detector Packages installed onto the GP-B telescope. Starlight is divided into four beams in the Image Divider. Two sets of beams are sent to the Detector Packages to control the pitch and yaw of the spacecraft.

2. DESIGN CONSIDERATIONS

The essential design problem is to thermally isolate a warm electronics assembly from the rest of a cryogenic telescope and Instrument. The telescope read-out electronics use silicon junction field-effect transistors (JFETs) because of their extremely low-noise characteristics. Unfortunately, Si JFETs do not operate reliably at temperatures less than 60 K. This is not welcome in a 2.5 K instrument where superconducting critical temperatures and cryogenic lifetimes are very important.

Table 1 lists some of the Detector Package requirements. The principal tasks are limiting the power dissipation to less than 1 mW per detector set while also achieving an adequately stiff support structure. Because the JFET amplification is temperature dependent, the temperature stability of the detector platform must be better than 2 mK. These requirements, and others, are made more difficult by the relatively narrow, annular volume allowed to the Detector Packages.

Table 1. Key GP-B Detector Package Requirements

Parameter		Required Value
Volume	Length	≤ 50 mm
	Width	≤ 18 mm
	Height	≤ 31 mm
Power Dissipation (4 dual photodiode detector sets)		≤ 4 mW (≤ 1 mW/detector set)
Platform Temperature	Operational	50–80 K
	Test	2–300 K
	Bakeout (survive)	340 K
Base Temperature	Operational	2–6 K
	Test	2–300 K
	Bakeout (survive)	340 K
Platform Temperature Variation		≤ 2 mK
Acceleration	First Resonance	≥ 100 Hz
	Random	3.6 g_{rms}
	Steady-state	TBD
Alignment	Pitch / Yaw	≤ 10 arc min
	Roll	≤ 30 arc min
	Defocus / Decenter	≤ 500 μm
Number of Electrical Leads		24
Electrical Lead Resistance		≤ 100 Ω

As shown in Table 1, the first resonance of the Detector Package and its sub-assemblies must be at least 100 Hz. Because the entire Instrument will be launched on a Delta II rocket, it must also survive a random vibration environment of 3.6 g_{rms}.

Alignment repeatability requirements for the Detector Package are 10 arc minutes in pitch and yaw, 30 arc minutes in roll. Defocus and decenter requirements are 500 μm. These alignment requirements must be maintained after the Instrument is cooled to its operating temperature, an excursion of 296 K.

Because of the extreme sensitivity of the GP-B gyroscope read-out sensor, the Detector Package also provides electromagnetic interference (EMI) shielding and has a low-remanent magnetic moment.

2.1 Materials

The evaluation of Isolator candidate materials started with commonly-used, low-temperature, low-conductivity materials. As shown in Table 2, thermal conductivities at cryogenic temperatures are considerably lower than at room temperatures. This is fortunate. While room temperature and cryogenic thermal conductivities generally track for various materials, we found two interesting exceptions.

Table 2. Thermal Isolator Candidate Materials

Temperature, K	Thermal Conductivity, W/m-K						
	Fused Quartz[4]	G-10 Graphite Epoxy[5]	Teflon[4]	Altex Graphite Epoxy[6]	Nylon 66[5]	Kapton HN[7]	Aerogel[8]
300	1.380	0.350	0.250	1.570	0.170	0.350	0.010
4	0.100	0.055	0.060	0.023	0.010	0.010	0.00001

The Altex graphite/epoxy composite has a thermal conductivity greater than fused quartz at room temperature. However, at 4 K, its thermal conductivity is less than that of teflon. Kapton, while no better than commonly-used G-10 graphite/epoxy at room temperatures, is 5.5 times better than G-10 at 4 K. We were only able to find one material with cryogenic thermal conductivity lower than kapton. While aerogel's 1000 times lower thermal conductivity is attractive, we do not currently have an aerogel-based design that meets the structural or electrical requirements. We should also mention the low thermal conductivity of nylon. While equal to kapton, its dimensional change ($\Delta L/L$) in going to LHe temperatures is 2 times that of kapton. Thus, kapton was chosen for its low thermal conductivity and acceptable $\Delta L/L$.

2.2 Structure

The power dissipation requirement of 1 milliwatt coupled with a vibration requirement of a 100 Hz fundamental frequency implies a light, stiff structure. We look to trusses and shells for their inherent efficiency. Our design goal is to find a structure that will thermally isolate one body from another body while providing adequate structural stiffness.

Truss structures can be configured in many space frame configurations. We initially considered straight-legged, rod-type stand-offs. These had unacceptably-low fundamental frequencies. Next we looked at the Stewart Platform. A Stewart Platform constrains exactly six degrees-of-freedom by using six struts attached at three points on one body and three points on a second body[9]. After some attempts to create an Isolator based on the Stewart Platform, fabrication and structural complications led us towards cylindrical shells.

Our thermal calculations immediately told us the cylinder would need to be thin-walled. We assumed the diameter to be roughly that of the Detector Circuit (9 mm). Even for a wall thickness of 50 μm, our thermal conductivity was 1.4 times too high. We decided to thermally lighten the cylinder by adding "windows". This left only three legs through which to transfer heat. By narrowing the legs and further decreasing the wall thickness of the cylinder to 38 μm, were able to theoretically meet our power dissipation requirement. Further, the chosen cylindrical Isolator geometry is more than 110 times stiffer than a square beam of equivalent cross-sectional area[10].

2.3 Alignment

The detector package is the final destination for the telescope light beam. When assembled to the telescope, the Package must align the detectors to the required accuracies (Table 1). Because of the desire to reinstall Packages without a complete telescope alignment test, the Detector Package should be designed to achieve the required accuracy through good mounting repeatability. In addition to achieving the alignment requirements, the Package must maintain these requirements after being cooled from room temperatures to LHe temperatures (ΔT=290 K). A kinematic coupling is appropriate[11].

3. APPROACH

3.1 Package

The design approach taken for the GP-B Detector Package is shown in Figure 3 below. A titanium housing encloses an optical sub-assembly consisting of a plano-convex lens and a beamsplitter. The plano-convex lens takes the two f/22 beams coming from the Image Divider and focuses them on the detector sets 12 mm away. The beamsplitter takes the f/5 light from the plano-convex lens and sends half to the primary detector set and half to a redundant detector set. Each Detector Mount is individually shielded to limit EMI from propagating to other sensitive subsystems in the Instrument.

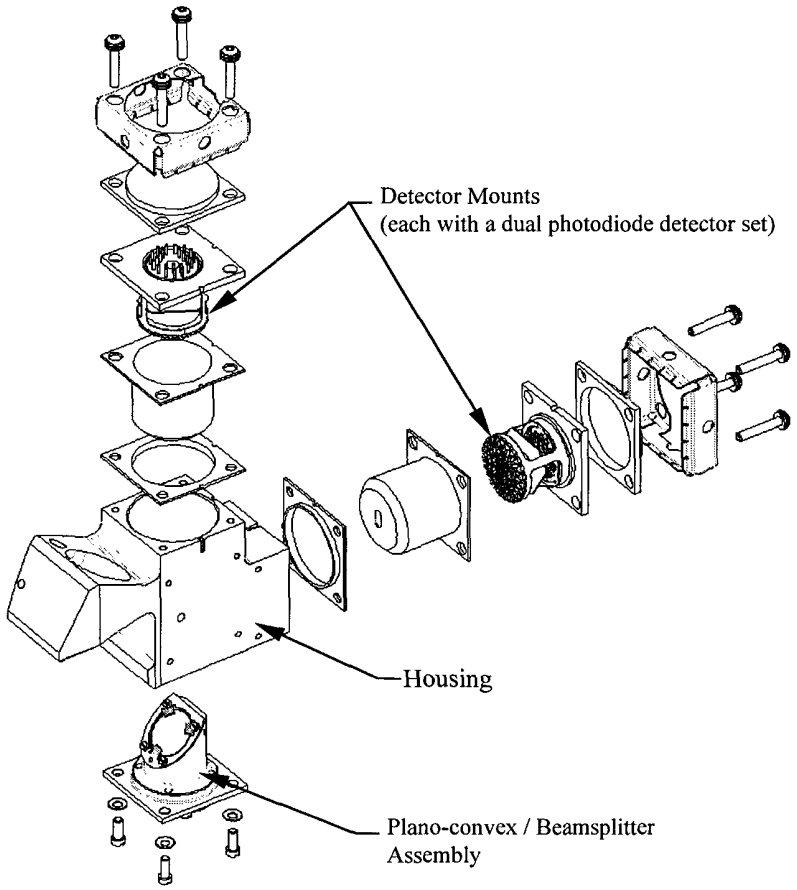

Figure 3 Exploded view of the Detector Package. The optical sub-assembly and Detector Mounts attach to a titanium housing Various EMI shields and electrical isolators are also shown

Figure 4 shows light from the Image Divider entering the Detector Package from below. As previously described, the light gets re-focused by the plano-convex lens then proceeds to the dual photodiode detector sets. The beamsplitter simply allows a redundant detector set in each Package. Also shown in Figure 4 is the semi-kinematic attachment scheme for the Detector Package to the telescope. A relatively broad flat, relieved in the center, constrains pitch, yaw, and defocus. A second, narrower flat constrains roll and x-decenter. Y-decenter is limited by the fit between the shoulder screw and the hole in the quartz post.

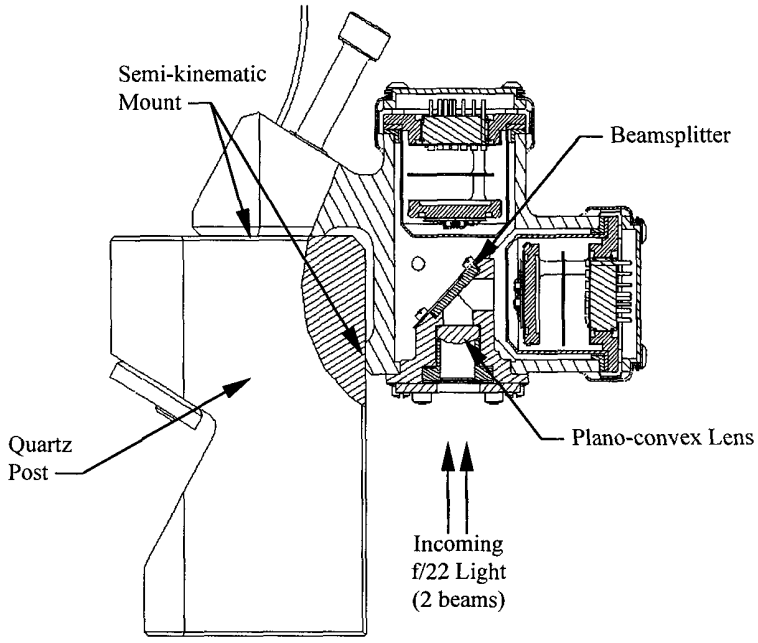

Figure 4 Side/section view of the Detector Package Light enters from underneath the Package through the plano-convex lens, which focuses the telescope light onto the detectors. Each Package has a redundant Detector Mount, achieved through use of a beamsplitter.

3.2 Mount

The Detector Mount (Figure 5) provides the thermal isolation necessary between the Detector Circuit and the rest of the telescope. The Circuit substrate is single-crystal sapphire to achieve the thermal stability requirement of less than 2 mK. The platform on which it sits is alumina.

The Isolator is 38 μm thick kapton polyimide film with copper/gold traces connecting the Circuit to the pins on the base. The 12 mm diameter and 11 mm height is compatible with the telescope packaging and vibration constraints.

The base is titanium for thermal compatibility with the housing. It is the interface to the rest of the Detector Package and the thermal ground for the Detector Mount.

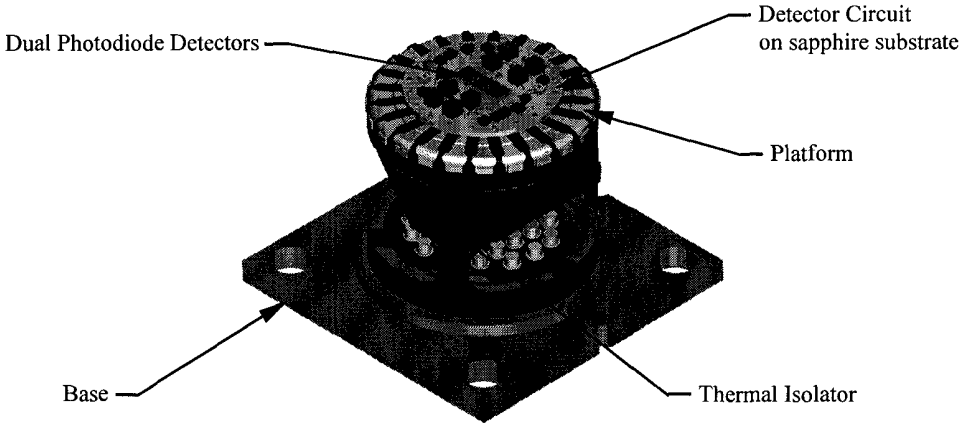

Figure 5 Detector Mount The dual photodiode detectors and JFETs are thermally sunk to a single-crystal sapphire substrate The substrate is mounted to a larger, alumina platform The platform is thermally isolated from the titanium base by a kapton thermal isolator.

3.3 Isolator

Figures 6 and 7 show the fabrication method for the Detector Mount. A standard piece of single-sided, copper-coated kapton film, commonly used in the flex circuit industry, is first coated on the uncoated side with a titanium/gold thin film. This is accomplished by either electron beam evaporation or sputtering. The ends of the Isolator are then selectively plated with 6 μm of gold to aid connections to the circuit and pins. Next, the Ti/Au traces are photo-fabricated. The Isolator part mechanical shape is then produced by either a reactive ion etching process through a copper mask or laser cutting using an excimer laser. The copper mask is finally removed with a preferential etch leaving the kapton Isolator with Ti/Au traces.

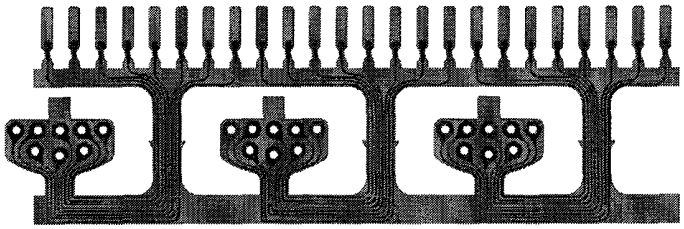

Figure 6. Thermal Isolator in flat form. The part starts as a sheet of copper-coated kapton. The 24 traces are made through a photolithography process. The part is cut out using ion etching or laser cutting.

The Isolator is then rolled into a cylinder and attached to the base (Figure 7). The 24 pins are indium soldered to the traces. The Isolator is then bonded to the base using epoxy. The rigidizer is snapped in and glued to the Isolator. The alumina platform is fit into the top of the cylindrical Isolator. The fingers and platform are bonded in one operation. After this sub-assembly has cured, the Detector Circuit is optically aligned and bonded using epoxy. Finally, wire bonds are made between the Circuit and the traces on the fingers. This completes the electrical connection between the photodiodes on the platform and the pin outs on the base. In between these connections are three legs that thermally isolate the electronics from the cryogenic telescope. This thermal isolation is accomplished while still providing adequate structural stiffness and stability.

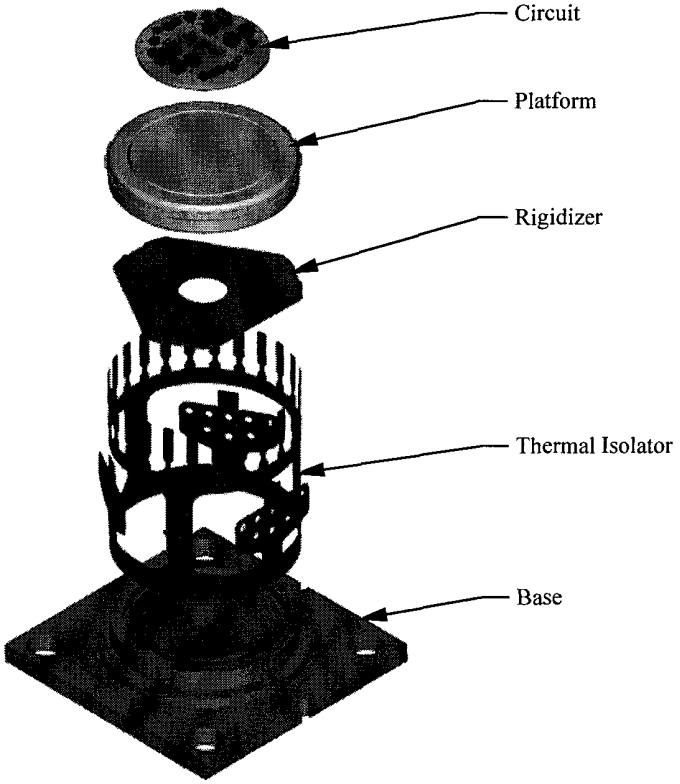

Figure 7 Exploded view of the Detector Mount.

3.4 Flex Cable

The thermal story is obviously not finished at the Detector Mount base. To bring the heat from the Detector Mount to an appropriate thermal sink, a multi-function Detector Cable is used. The cable has three simultaneous functions:

- electrical connection between the 24 pins on the Detector Mount and the connector on the dewar probe,
- thermal connection between the Detector Mount base and the LHe dewar,
- EMI shielding between the detector signals and other extremely sensitive components in the Science Instrument.

The construction of the Detector Cable is also based on flex circuit technology. The 24 electrical connections are first photo-fabricated on a sputtered, copper-coated kapton film. The back of this kapton film is also copper-clad and provides local EMI shielding. Layers of acrylic adhesive are then added to both sides of this copper/kapton/copper construction. Bonded to each side is another kapton/copper film providing RF shielding. The outer, exposed copper layers are finally covered with a protective layer of kapton, again held on by an acrylic adhesive layer on each side. Coating thermal contact surfaces with malleable indium or gold coatings minimizes thermal contact resistances[12]. This multi-function flex cable is 0.5 mm thick and 8 mm wide. Custom fabrication for each Detector Mount ensures a proper routing to a micro D connector, as well as low forces and moments imposed on the quartz, telescope detector post.

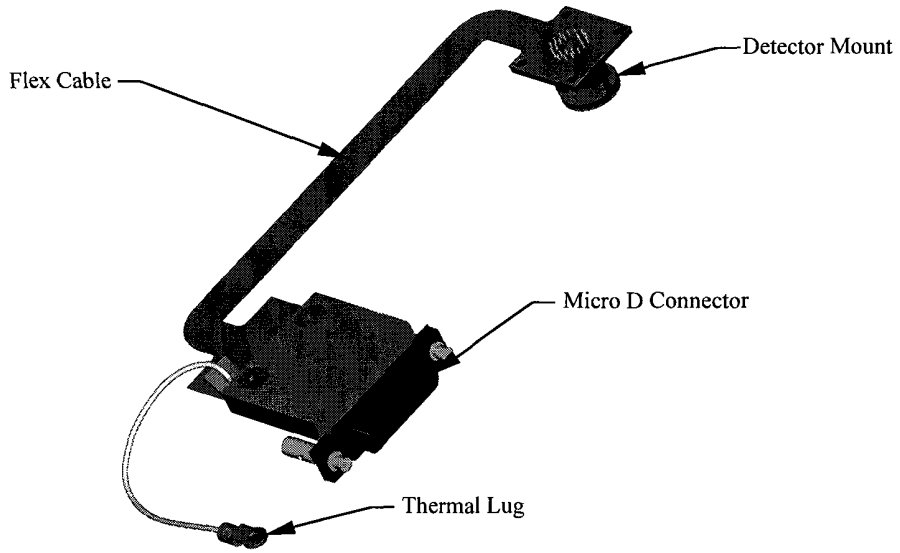

Figure 8. Detector Flex Cable The Flex Cable provides electrical connection between the Detector Mount and its Circuit and the connector to the telescope read-out electronics modules It also acts as a thermal ground strap and incorporates EMI shielding.

4. ANALYSES

We made use of simple 1-D conduction and radiation models to help choose geometry and materials. The conduction model was set up in a spreadsheet and used to verify our initial design. The spreadsheet looked at each of five segments of the Isolator and determined an average thermal conductivity based on the temperatures at the ends of the segments. This gave us approximate thermal isolator leg dimensions. Thermal conduction results from our first simple prototypes came within a factor of two of our models. The 1-D conduction spreadsheet was later verified with a joint conduction/radiation spreadsheet model. More detailed models, using finite element analyses, are planned to help us understand the subtleties of the Isolator behavior. We also plan to expand the model to account for the thermal impedances provided by the telescope connections and the Detector Cable.

Finite element analyses have predicted a fundamental frequency of the Detector Mount in excess of 400 Hz. This has been qualitatively verified by tapping the completed assemblies. As long as the Isolator is not buckled, the cylindrical structure is remarkably stiff. While encouraging, we have also seen the legs of the thermal isolator flatten towards the middle of their span. This is Saint-Venant's principle reminding us that as we move away from the boundary conditions, the material tends to forget our efforts to make it cylindrical[13]. The concern is that if the legs flatten, and cease to act as portions of a cylinder, the fundamental frequency could drop significantly. The Isolator would also be more likely to buckle. To counter this effect, a thin rigidizer has been placed inside the Isolator to maintain the shape of the legs (i.e., imposing a cylindrical boundary condition). By putting the rigidizer in the middle of the Isolator, away from the platform and base, the only thermal short is across the width of the rigidizer (small).

5. TESTING

Extensive inspection and electrical testing are performed on Isolators before they are committed to a Detector Mount. Electrical resistance measurements are taken for each trace. Microscopic inspection at 10 to 90 power magnification is done to check the Isolator and traces for cracks, scratches, or other defects. When a Detector Mount is completed, a final end-to-end test for continuity and isolation is performed on each trace. The Detector Circuit is pre-screened and operated at liquid nitrogen temperature, 77 K, before the Circuit is aligned and permanently bonded to the Detector Mount.

6. RESULTS

To date, we have built four functioning units with a previous four-leg design. A plot of the measured platform temperature as a function of total power dissipation is shown below in Figure 9.

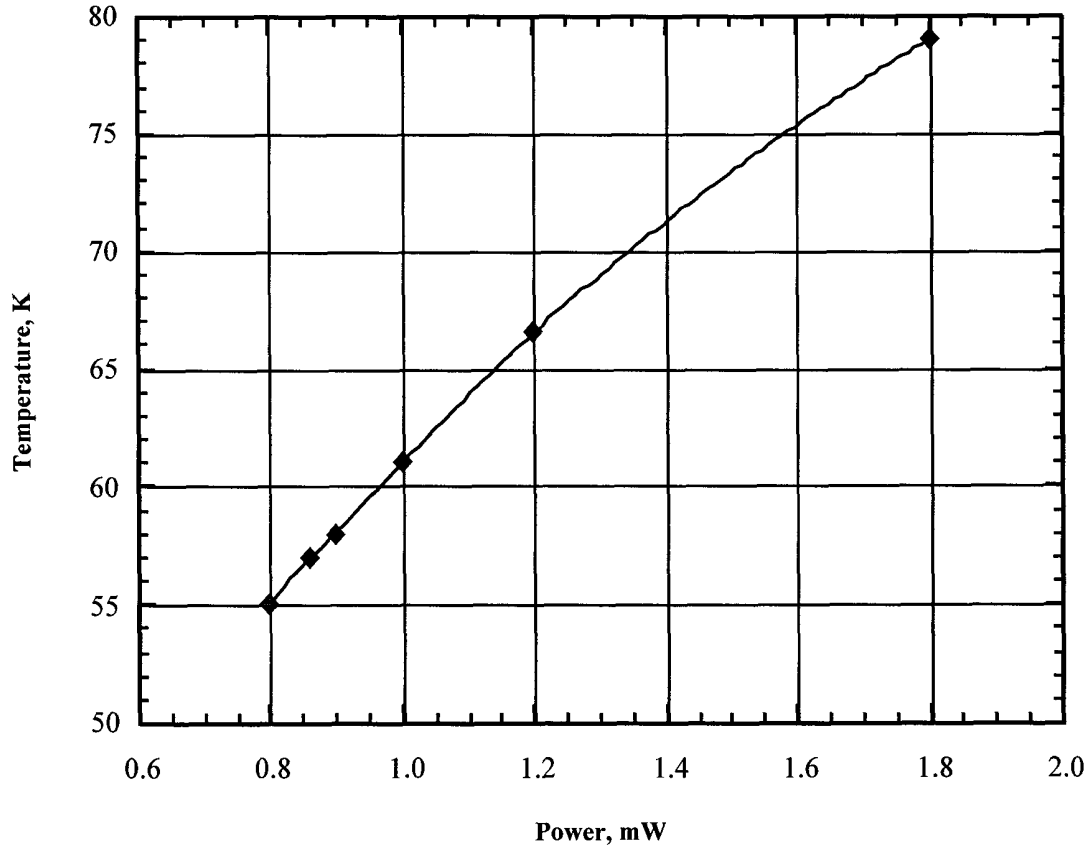

Figure 9. Plot of Detector Circuit temperature vs power input. We currently reach 61 K for 1 mW of power dissipation

The total power dissipation on the Circuit is the sum of the photo-detection circuit and a heater resistor. The Circuit dissipates 0.8 mW of power and the balance is provided by the heater resistor. During flight, the heater can be operated from 0 to 0.2 mW. Because the JFET noise characteristics and gate leakage current are temperature dependent, it would be desirable to have a wider temperature range in which to find an optimum operating point. From the graph, it is evident that we can operate between 55 K and 61 K and stay within our 1 mW requirement. The current three-leg design should show improved isolation and an increased operating range.

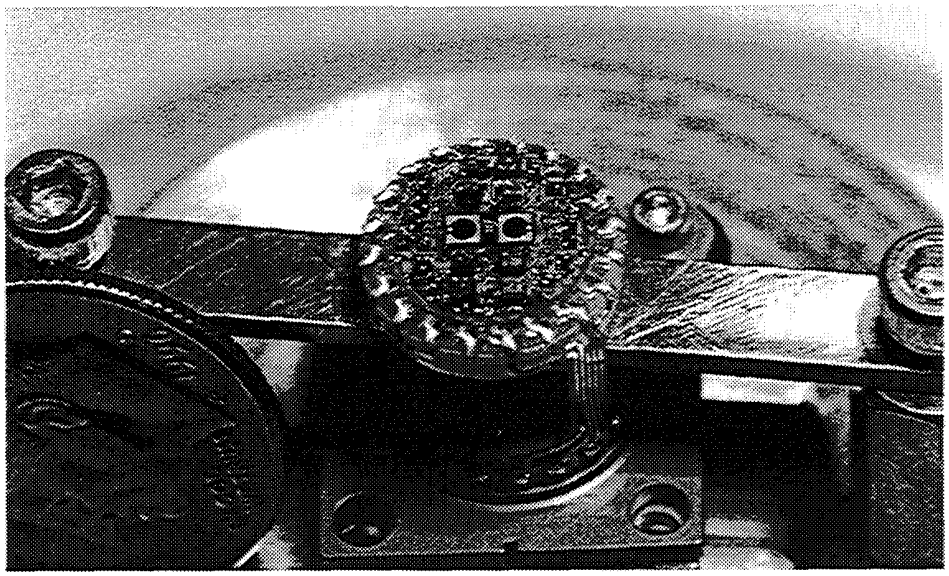

Figure 10. Photo of a Detector Mount in an assembly fixture

7. SUMMARY

We have designed, built, and tested a detector mount system which provides 1 mW of thermal isolation between temperatures of 61 K and 2 K. We are working to improve the thermal isolation of this detector mount system to less than 1 mW for a 78 K temperature differential. This mount system appears adequate for use in space-borne applications and will be demonstrated as work continues. The critical Thermal Isolator employs techniques common to the flex circuit industry. The Detector Cable is a multi-layer flex circuit providing electrical connections, EMI shielding, and thermal strapping in one, compact package. Because of the criticality of this application, we have provided redundancy in the Package through use of a beamsplitting optic, allowing redundant detector sets. By employing a semi-kinematic mount between the Detector Package and the telescope, it is possible to change out a Detector Package without a complete re-alignment of the telescope optical system. This detector mount system allows use of silicon JFETs in a LHe instrument. These extremely low-noise JFETs make possible a telescope read-out system with 10 milli-arc second/$\sqrt{\text{Hz}}$ random noise. The telescope read-out must be stable to 5 electrons/second to achieve its 50 micro-arc seconds of pointing stability requirement. The Detector Mount's thermal isolation and stability are key to achieving this.

8. ACKNOWLEDGMENTS

The authors are grateful to Bob Farley, Ken Bower, John Turneaure, Ken Coleman, Jason Gwo, Ben Taller, Larry Novak, Nick Scott, and Jeff Wade for their help and encouragement throughout this effort. This work is supported by the National Aeronautics and Space Administration, Marshall Space Flight Center, under contract NAS8-39225.

9. REFERENCES

1. J. P. Turneaure, et al., "Development of the Gravity Probe B Flight Mission", *Adv. Space Res.*, 1996.

2. B. Muhlfelder, J. M. Lockhart, G. M. Gutt, "The Gravity Probe B Gyroscope Readout System", *Adv. Space Res* , 1996.

3. D.-H. Gwo, et al., "The Gravity Probe B Star-Tracking Telescope", *Adv Space Res.*, 1996.

4. Touloukian, et al., *Thermophysical Properties of Matter*, Volumes 1-3, Plenum Press, 1970-1973.

5. Lake Shore Cryotronics, Inc., "Cryogenic Heat Flow Calculations", Publication C2S107A.

6. D. L. Rule, L. L. Sparks, "Low-Temperature Thermal Conductivity of Composites: Alumina Fiber/Epoxy and Alumina Fiber/PEEK", NISTIR 89-3914, National Institute of Standards and Technology, May 1989.

7. D. L. Rule, D. R. Smith, L. L. Sparks, "Thermal Conductivity of a Polyimide Film between 4.2 and 300 K, with and without Alumina Particles as Filler", NISTIR 3948, National Institute of Standards and Technology, August 1990.

8. T. Squire, "Thermal Protection Systems Expert and Material Properties Database", NASA Ames Research Center, 1997.

9. B. Borchardt, R. Hartsock, F. Rudder, D. Sawyer, "Hexapod Metrology", NISTIR 5885, National Institute of Standards and Technology, 1996.

10. R. J. Roark, W. C. Young, *Formulas for Stress and Strain*, McGraw-Hill Book Company, 1975.

11. S. T. Smith, D. G. Chetwynd, *Foundations of Ultraprecision Mechanism Design*, Gordon and Breach Science Publishers, 1992.

12. L. J. Salerno, P. Kittel, "Thermal Contact Conductance", NASA Technical Memorandum 110429, February 1997.

13. J. P. Den Hartog, *Advanced Strength of Materials*, pp. 117-118, McGraw-Hill Book Company, 1952.